



Published in final edited form as:

Int J Pharm. 2020 September 25; 587: 119623. doi:10.1016/j.ijpharm.2020.119623.

Trans-urocanic acid enhances tenofovir alafenamide stability for long-acting HIV applications

Antons Sizovs^a, Fernanda P. Pons-Faudoa^{a,b}, Gulsah Malgir^{a,c}, Kathryn A. Shelton^d, Lane R. Bushman^e, Corrine Ying Xuan Chua^a, Peter L. Anderson^e, Pramod N. Nehete^{d,f}, K. Jagannadha Sastry^{d,g,h}, Alessandro Grattoni^{a,i,j,*}

^aDepartment of Nanomedicine, Houston Methodist Research Institute, Houston, TX 77030, USA

^bTecnologico de Monterrey, School of Medicine and Health Sciences, Monterrey, NL, Mexico

^cDepartment of Biomedical Engineering, University of Houston, Houston, TX 77204, USA

^dDepartment of Comparative Medicine, Michael E. Keeling Center for Comparative Medicine and Research, MD Anderson Cancer Center, Bastrop, TX 78602, USA

^eDepartment of Pharmaceutical Sciences, Skaggs School of Pharmacy and Pharmaceutical Sciences, University of Colorado- Anschutz Medical Campus, Aurora, CO 80045, USA

^fThe University of Texas Graduate School of Biomedical Sciences at Houston, Houston, TX 77030, USA

^gDepartment of Thoracic Head and Neck Medical Oncology, University of Texas MD Anderson Cancer Center, Houston, TX 77030, USA

^hThe University of Texas MD Anderson Cancer Center UTHealth Graduate School of Biomedical Sciences at Houston, Houston, TX 77030, USA

ⁱDepartment of Surgery, Houston Methodist Research Institute, Houston, TX 77030, USA

^jDepartment of Radiation Oncology, Houston Methodist Research Institute, Houston, TX 77030, USA

Abstract

Long-acting (LA) pre-exposure prophylaxis (PrEP) for HIV prevention is poised to address nonadherence and implementation challenges by alleviating the burden of user-dependent dosing. Due to its potency, tenofovir alafenamide (TAF) is a viable candidate for LA PrEP. However, the

*Corresponding author. agrattoni@houstonmethodist.org.

Author contributions

Antons Sizovs: conceptualization, methodology, formal analysis, investigation, writing-original draft preparation. **Fernanda P. Pons-Faudoa:** formal analysis, investigation, writing-review and editing, visualization. **Gulsah Malgir:** investigation. **Kathryn A. Shelton:** investigation. **Lane R. Bushman:** methodology, validation, investigation. **Corrine Y. X. Chua:** formal analysis, writing-review and editing. **Peter L. Anderson:** methodology, validation, resources, writing-review and editing. **Pramod N. Nehete:** investigation, resources, project administration, writing-review and editing. **K. Jagannadha Sastry:** conceptualization, resources, writing-review and editing. **Alessandro Grattoni:** conceptualization, investigation, resources, writing-original draft preparation, writing-review and editing, visualization, supervision, project administration, funding acquisition.

Publisher's Disclaimer: This is a PDF file of an unedited manuscript that has been accepted for publication. As a service to our customers we are providing this early version of the manuscript. The manuscript will undergo copyediting, typesetting, and review of the resulting proof before it is published in its final form. Please note that during the production process errors may be discovered which could affect the content, and all legal disclaimers that apply to the journal pertain.

inherent hydrolytic instability of TAF presents a challenge for application in LA systems. In this work, we examined the mechanism of TAF hydrolysis in a reservoir-based implant system and characterized TAF degradation kinetics as a function of the solution pH. We determined a pH “stability window” between pH 4.8 – 5.8 in which TAF degradation is substantially mitigated, with minimal degradation at pH 5.3. In a pursuit of a TAF formulation suitable for LA PrEP, we studied *trans*-urocanic acid (UA) as a buffer excipient. Here we show that UA can maintain the pH of TAF free base (TAF_{fb}) solution inside a surrogate implant model at approximately pH 5.4. Through in vitro analysis, we demonstrated preservation of released TAF purity above 90% for over 9 months. Further, we performed an in vivo assessment of TAF_{fb}-UA formulation in a reservoir-based nanofluidic implant inserted subcutaneously in non-human primates. Preventive levels of tenofovir diphosphate above 100 fmol/10⁶ peripheral blood mononuclear cells were achieved in 2 days and sustained over 35 days. Fluid retrieved from implants after 60 days of implantation showed that UA preserved the aqueous phase in the implant at ~pH 5.5, effectively counteracting the neutralizing action of interstitial fluids. Moreover, residual TAF in the implants maintained >98% purity. Overall, TAF-UA represents a viable formulation applicable for LA HIV PrEP.

Keywords

long-acting drug delivery; HIV PrEP; implants; drug formulation

1. Introduction

Advances in antiretroviral therapy (ART) for pre-exposure prophylaxis (PrEP) have dramatically transformed the landscape of HIV prevention. Specifically, Truvada® (200 mg emtricitabine/300 mg tenofovir [TFV] disoproxil fumarate [TDF]) and Descovy® (200 mg emtricitabine/25 mg tenofovir alafenamide fumarate salt [TAF_{fs}]) are United States Food and Drug Administration (FDA) approved oral ART pills for HIV PrEP. PrEP efficacy is tightly linked with adherence to once-a-day regimen. With seven daily doses per week, PrEP is nearly 100% effective in curbing sexual HIV transmission in men or transgender women who have sex with men^{1,2}, while two daily doses per week reduces prevention rate to 76%. Further, according to the Centers for Disease Control and Prevention, only approximately <5% of high-risk individuals who stand to benefit have initiated PrEP^{3,4}. These PrEP adherence and implementation challenges, including limited medical access, have galvanized research endeavors into devising long-acting (LA) formulations or platforms that obviate the need for user-dependent daily dosing⁵⁻⁹.

LA formulations or controlled release implants offer prolonged delivery in a sustained manner to ensure continuity of exposure to the drug¹⁰⁻¹². To maximize drug loading while maintaining low volume for injectables or implants, research efforts are predominantly focused on the use of a single drug. To this end, TAF has emerged as a prime candidate for LA injectables or implants because of its superior potency at a lower dose^{13,14} and safety profile¹⁵ compared to TDF. However, fundamental to the successful implementation of LA TAF is overcoming the challenge of poor hydrolytic stability¹⁶. TAF free base (TAF_{fb}) readily loses its phosphonic acid protective groups and has a short half-life of 1.3 days at

physiological conditions (pH 7.4 and 37 °C). Of paramount importance, development of LA systems requires TAF to be stable in the body and maintain biological activity throughout the intended duration of administration, ideally for months to years. As such, formulation-based approaches are at the forefront of efforts directed at improving TAF stability in LA systems.

Recognizing the potential of TAF for HIV PrEP, numerous LA strategies are under preclinical investigations. One strategy developed by Gunawardana et al. entails a subdermal implant with TAF_{fb} loaded into a silicone tubing without excipients and a polyvinyl alcohol membrane for controlled release¹⁷. The subcutaneous LA implant developed by Su et al. involves granulating TAF fumarate salt (TAF_{fs}) with NaCl (2%, w/w) and dry-coating with sodium stearate (2%, w/w)¹⁸. The resulting pellets were incorporated into a medical-grade polyurethane tube, where the tube wall acts as a reservoir while the polyurethane membrane controls drug release. Excipient-based formulations were pursued by Johnson et al. using castor oil to disperse TAF_{fb} in a poly(caprolactone) implant¹⁹, whereas Schlesinger et al. used PEG3000²⁰. These reports showed that hydrolysis products inside the reservoir comprise less than 10% of the total drug after extended periods of release. However, the reported composition of the residual drug was universally measured by assessment of all of the remaining content, including solids. To the best of our knowledge, the stability of the solubilized drug in the implant or purity of released TAF was not evaluated. Nevertheless, collectively, these studies underscore that hydrolysis is a key factor in poor TAF stability, regardless of its fumarate or free base form, emphasizing the need for stable formulations.

In this work, we first investigated the parameters affecting TAF_{fb} stability in a reservoir-based implant model and evaluated the mechanism of TAF degradation in vitro. We attributed the hydrolytic instability of TAF to be dependent on pH in the implant microenvironment. To improve drug stability, we rationally selected urocanic acid (UA), a molecule endogenously abundant in the human skin²¹, as an excipient for TAF_{fb} in LA platforms. UA has pH buffering properties²² and unlike typical pH buffers, presents low solubility comparable to TAF_{fb}. This allows UA to be released from the implant with similar release kinetics as TAF_{fb}, while maintaining stable pH conditions within the range of 5.2 to 5.4 in the implant for a long duration. As a result, UA minimizes TAF degradation, as we demonstrated for at least 9 months in vitro. To validate our finding, we assessed TAF_{fb}-UA stability in our reservoir-based nanofluidic implant in non-human primates (NHP).

2. Materials and methods

2.1 Materials

All materials and reagents were purchased from Fisher Scientific (Hampton, NH) unless otherwise noted. TAF_{fs} was provided by Gilead Sciences, Inc. (Foster City, CA).

2.2 HPLC analysis of TAF degradation

High performance liquid chromatography (HPLC) analyses were performed using Hitachi Chromaster instrument equipped with UV-Vis photodiode array detector and a 3.5 µm 4.6×150 mm Eclipse Plus C18 column. HPLC analyses were performed using 25 µL

injections with ammonia acetate buffered water (solvent A) and methanol (B) gradient: 5% B (0 min), 5% B (0.8 min), 100% B (3.8 min), 100% B (4.6 min), 5% B (5.2 min) at 2.000 mL/min flow rate. Chromatograms were recorded at absorbance maximum of 260 nm. All peaks corresponding to TAF_{fb} and its hydrolysis products were integrated. TAF purity was calculated as % TAF_{fb} peak area relative to the sum of TAF_{fb} and its hydrolysis products.

2.3 TAF hydrolysis constant dependence on pH

A series of buffered solutions were prepared by combining 0.1 M sodium citrate and 0.2 M sodium dihydrogen phosphate solutions at different ratios. Each vial contained 2.7 mL of respective buffer solution. A 0.3 mL aliquot of fresh 1.0 mg/mL TAF_{fb} solution in deionized (DI) water was added to each vial. Vials were placed on a shaker at 37 °C for the solutions to equilibrate for 3 h. After 3, 27, 51, and 75 h, pH of the solutions was measured with a pH meter. 25 µL of each solution was removed and analyzed by HPLC. Hydrolysis constants were determined by linear fitting of the $\ln([TAF_{fb}]_t/[TAF_{fb}]_0)$ versus time, t .

2.4 TAF stability from in vitro release

To evaluate TAF_{fb} purity in the efflux between differently formulated drugs, we used centrifugal filter tubes equipped with a nylon membrane with 20 nm porosity as surrogates for reservoir-based implants (Figure 1). Filter membranes were primed by centrifuging (500 g for 2 min) 1X phosphate-buffered saline (PBS) through the membrane. Each reservoir was loaded with 100 mg TAF_{fs}, 100 mg TAF_{fb}, or 600 mg of TAF_{fb}-UA formulation at 2:1 ratio (w/w) in powder form and filled with PBS. Thereafter, to ensure complete air removal, reservoirs were centrifuged (500 g for 2 min), filled with PBS and capped. To avoid leakage, the seam between the reservoir and cap was glued with acrylonitrile glue. Implants were fitted and glued into hole-punched scintillation caps. Each scintillation vial was equipped with a Teflon-coated magnetic stir bar and filled with 22.00 mL of PBS, serving as the sink solution. Assembled vials were placed on a stirrer at 37 °C. Every 48 h, the sink solution was entirely retrieved and replaced with 22 mL of fresh pre-warmed PBS. 500 µL were used for analysis. Retrieved sink solutions were analyzed via HPLC as described in 2.2. To evaluate the purity of released TAF_{fb}, the hydrolysis occurring within the sink reservoir was considered. TAF % purity fraction was obtained from the ratio between the release rate of TAF_{fb} (RR_{TAF}) and the total release rate (RR_{Total}), inclusive of both TAF_{fb} and all degradation products. RR_{Total} was obtained directly from HPLC peak integration, while RR_{TAF} was calculated as follows:

$$\frac{d(nTAF_{fb})}{dt} = RR_{TAF} - nTAF_{fb} \times k_H \quad [1]$$

which in its integral form leads to:

$$nTAF_{fb} = \frac{RR_{TAF_{fb}}}{k_H} (1 - e^{-k_H \times t}) \Rightarrow RR_{TAF_{fb}} = \frac{nTAF_{fb} \times k_H}{(1 - e^{-k_H \times t})} \quad [2]$$

where $nTAF_{fb}$ is the amount of TAF_{fb} [mols] present in the sink solution at any given time, t is time [day]; RR_{TAF} is expressed as mols/day, k_H is the hydrolysis rate constant in PBS solution [day^{-1}], and V_{sink} is the volume of sink solution [L].

2.5 Implant assembly for in vivo study

Flat elongated 6Al4V titanium implants with a 570.0 mm³ drug reservoir were used for TAF_{fb}-UA release study in rhesus macaques. A biocompatible, SiC-coated nanofluidic membrane with 150 nm nanochannels was mounted within each implant. Further details on the membrane microfabrication, analysis and implant structure are available in literature²³. In these membranes, nanochannels control diffusive drug release via physical and electrostatic confinement on drug molecules, obtaining a saturated and sustained trans-membrane transport^{12,24,25}. Implants were assembled in a sterile field as previously described²⁶. Briefly, implants were cleaned, autoclaved and kept in aseptic conditions during the assembly and drug loading steps. Membranes were epoxied (EPOTEK 0G116-31) within the implant drug chambers and UV-cured. Devices were loaded with ~300 mg of TAF_{fb}-UA. Implants were welded to ensure a tight seal. Thereafter, implants were then immersed in sterile PBS and primed by applying and releasing vacuum three times, consecutively.

2.6 Non-human primate (NHP) model studies and implantation procedure

The TAF_{fb}-UA stability study using rhesus macaques as the NHP model was conducted at the Michale E. Keeling Center for Comparative Medicine and Research, The University of Texas MD Anderson Cancer Center (UTMDACC), Bastrop, TX. The UTMDACC center is accredited by the Association for Assessment and Accreditation of Laboratory Animal Care-International (AAALACI). The animal studies were performed in compliance with the requirements of the Animal Welfare Act, PHS Animal Welfare Policy, and the principles of the NIH Guide for the Care and Use of Laboratory Animals. All procedures were approved by the Institutional Animal Care and Use Committee at UTMDACC. Male rhesus macaques of Indian origin (*Macaca mulatta*; n=4) at 5 years of age, ranging between 7-10 kg, from the Specific Pathogen Free breeding colony at this facility were used in the study. Animals had access to clean, fresh water ad libitum and were fed a standard laboratory diet.

All procedures were performed under anesthesia with ketamine (10 mg/kg, intramuscular) and phenytoin/pentobarbital (1 mL/10 lbs, intravenous [IV]). The device implantation procedure was performed as follows: A 10 mm dorsal skin incision was made on the right lateral side of the thoracic spine followed by a ventral subcutaneous blunt dissection. Each animal received an implant, which was inserted into the subcutaneous pocket at an approximate depth of 5-cm from the skin incision, with the drug eluting membrane oriented towards the body. 4-0 polydioxanone (PDS) suture was used to close the pocket and completed intradermally for closure of the incision. All animals were administered one 50,000 U/kg perioperative penicillin G benzathine/penicillin G procaine (Combi-Pen) injection and daily meloxicam (subcutaneous, 0.2 mg/kg on day 1 and 0.1 mg/kg on days 2 and 3) to treat post-surgical pain.

2.7 Macaque blood collection and peripheral blood mononuclear cells sample preparation

Intracellular tenofovir diphosphate (TFV-DP) levels were measured in peripheral blood mononuclear cells (PBMC) pre-implantation and on day 1, 2, 3, 7, 14, 21, 28, and 35 post-implant insertion. PBMC isolation from blood collected in EDTA-coated vacutainer tubes was completed via Ficoll Hypaque centrifugation as previously described²⁶. Cells (viability above 95%) were counted, pelleted by centrifugation ($400 \times g$, 10 min), diluted in 500 μL of cold 70%:30% methanol: water solution, and kept frozen at -80°C until analysis.

2.8 Measurement of intracellular TFV-DP PBMC concentration

Intracellular TFV-DP concentrations in PBMC were quantified using previously described validated liquid chromatographic-tandem mass spectrometric (LC-MS/MS) analysis^{2,27}. The lower limit of quantitation (LLOQ) was 25 fmol/sample. However, in the case sample required higher sensitivity, a 5 fmol/samples LLOQ was used, as previously described²⁷.

2.9 Device retrieval and evaluation of TAF stability

Enterobacter cloacae was unexpectedly detected in fluids surrounding implants on day 49 postdeployment, which was non-impactful to study endpoints. The fluid analysis was performed in response to a mild swelling that was observed surrounding the implants post day 35. The swelling was likely due to the bacterial infection. Swelling could also be ascribed to subcutaneous tissue response to TAF_{fb} . While this has been previously reported¹⁸, we did not observe it in our previous study with subcutaneous TAF_{fs} implants^{26,28}. In light of the swelling, we decided to limit the PBMC results from the time of implantation to the time point before the first sign of enterobacterial infection appeared. This was done to conservatively avoid any potentially confounding effect of the infection in the results presented. Thus TFV-DP levels in PBMCs were followed for 35 days, whereas implants were surgically retrieved in a survival surgery 63 days after implantation. Approximately 50 μL of drug solution was aspirated with a syringe from the reservoir to evaluate TAF_{aq} and TAF_{s} . A pH 4.0 – 7.0 indicator strip was dipped in MilliQ pore water and gently agitated to remove excess water. A drop of drug solution was placed on pH indicator strip and the color was compared to reference color values. Remaining drug solution was retrieved from the implants and stored at -80°C until HPLC analysis. Devices were stored in ethanol (70%, w/w).

Drug solution was thawed over ice, filtered with a 0.02 μm centrifugation filter and diluted 100 times with 1X PBS. TAF_{s} stability was assessed by extracting the entire reservoir contents in ethanol (70%, w/w), filtered with a 0.02 μm centrifugation filter and diluted 100 times with Millipore water. TAF_{aq} and TAF_{s} were analyzed via HPLC as aforementioned.

3 Results and discussion

3.1 TAF solubility vs pH

Most reservoir-based drug delivery implants under development use TAF_{fb} or TAF_{fs} in solid form (TAF_{s}) alone (Fig. 2A) or mixed with an excipient. This allows for maximizing drug loading efficiency and stability, while minimizing implant volume. First, we consider the

scenario of TAF_S alone without excipient. Once an implant is surgically inserted subcutaneously, interstitial fluid penetrates the drug reservoir via capillary wetting of the controlled-release membrane, dissolving a portion of the drug (TAF_{aq}).

Thereafter, an equilibrium between TAF dissolution and precipitation is formed, defined by the solubility constant $K_s = 0.015 \text{ M}$ (7.15 mg/mL). TAF_{fb} is a weak base and in aqueous solutions exists in an equilibrium between its neutral and protonated forms: $\text{TAF}_{\text{aq}} + \text{H}^+ \rightleftharpoons \text{TAFH}^+_{\text{aq}}$ (pKa=3.96). TAF_{fb} solubility is dependent on the pH of the solution and increases rapidly when pH approaches its pKa, due to the significant contribution of protonated TAFH⁺ (Fig. 2B). Additionally, the kinetics of TAF release from the implant is slower than the dissolution kinetics. Therefore, after an initial transient phase, steady state conditions are established within the implant, in which the concentration $c(\text{TAF}_{\text{aq}})$ of dissolved TAF remains constant and nearly equal to its solubility:

$$c(\text{TAF}_{\text{aq}}) = [\text{TAF}_{\text{aq}}] + [\text{TAFH}^+] = K_s + \frac{[\text{TAF}][\text{H}^+]}{K_a} = K_s \left(1 + \frac{\text{pH}}{\text{pK}_a} \right) \quad [3]$$

where k_a is the acidity constant of the conjugate acid TAFH⁺

$$K_a = \frac{[\text{H}^+][\text{TAF}_{\text{aq}}]}{[\text{TAFH}^+]} \quad [4]$$

and k_s is the solubility constant of TAF_{aq}

$$K_s = [\text{TAF}_{\text{aq}}]. \quad [5]$$

3.2 TAF hydrolysis

Reaction of phosphoramidate esters such as TAF_{fb} with water can be initiated by water molecules, H⁺, or OH⁻ ions. This hydrolysis reaction proceeds through different pathways leading to various intermediate products of degradation and finally, to tenofovir (TFV). The pH of the solution determines the dominant hydrolysis pathway¹⁶. In this study, we defined the rate of hydrolysis, k_H as the rate of TAF_{fb} loss, related to the initial hydrolysis step, regardless of the hydrolysis mechanism. Hydrolysis of both TAF_{fb} and TAFH⁺ leads to loss of starting material, and k_H can be expressed as:

$$[\text{TAF}_{\text{aq}}] \times k_{H1} + [\text{TAFH}^+] \times k_{H2} = [\text{TAF}_{\text{aq}}] \times \left(k_{H1} + k_{H2} \times \frac{\text{pH}}{\text{pK}_a} \right) = [\text{TAF}] \times k_H \quad [6]$$

where k_{H1} and k_{H2} are the hydrolysis constants for TAF_{fb} and TAFH⁺, respectively.

To experimentally measure rates of TAF_{fb} hydrolysis, we employed a series of citric acid/phosphate buffers at 37 °C. A low TAF_{fb} concentration (0.10 mg/mL) was adopted as TAF_{fb} hydrolysis produces phosphonic acid (TFV), which is a strong acid that can alter pH of the solution at higher concentration. Measured k_H values as a function of pH of the solution are shown in Figure 3A, B.

Decomposition of TAF_{fb} appears to be significantly more sensitive to [OH⁻] than to [H⁺], as the hydrolysis rate increases rapidly above pH of 6. A “stability window” between pH 4.5 – 6.0 is observed with corresponding hydrolysis rate constants below 0.050 day⁻¹ (Fig. 3A, B). k_H data within the stability window were fitted using the equation $k_H = a \times [H^+] + b \times [OH^-] + c$ to highlight the contribution of [H⁺], [OH⁻] and H₂O to TAF hydrolysis. Values of $a = 10^3$, $b = 3.24 \times 10^6$, and $c = 0.0132$ were obtained. The fitting curve is shown in Figure 3B. The minimum theoretical value for $k_H = 0.025 \text{ day}^{-1}$ was analytically obtained, corresponding to pH 5.24.

While the rate of hydrolysis and TAF_{fb} solubility depend on pH, the total amount of hydrolyzed byproducts (TFV*) depends linearly on the volume of the aqueous phase inside the implant reservoir, V_{aq} . The rate of TFV* generation (R_{TFV^*}) is shown in Figure 3C as a function of V_{aq} . While R_{TFV^*} is high at physiological conditions (pH 7.4), TFV* generation is significantly mitigated (~16.4 fold) at pH 5.3, approximately corresponding to the theoretical minimum value. These results clearly indicate that minimizing V_{aq} via rational implant design represents a viable strategy to limit TAF_{fb} degradation. However, for implants possessing a rigid reservoir, V_{aq} will increase as drug is released and depleted from the reservoir. As such, to achieve long term stability of TAF_{fb} in the implant, a formulation capable of maintaining pH 5.3 for the lifespan of the implant is needed.

3.3 TAF free base vs TAF fumarate salt.

Although it is FDA-approved for oral use as an active ingredient in Descovy®, TAF_{fs} presents properties that limit its use in implants. TAF_{fb} is a weak base with $pK_a = 3.96$, whereas fumaric acid has $pK_{a1} = 3.03$ and $pK_{a2} = 4.44$. Consequently, aqueous solutions of TAF fumarate are acidic at a pH of 3.6, corresponding to TAF_{fb} solubility of 23 mg/mL. TAF free base has no buffering capacity near physiological pH and therefore the pH of its saturated solution (7.0 mg/mL at 37 °C) is determined by other ions. However, hydrolysis of TAF_{fb} acidifies the solution due to formation of phosphonic acid (TFV). As a result, hydrolysis at pH values above 5.3 is a self-inhibiting process.

To experimentally investigate the difference in stability between TAF_{fb} and TAF_{fs}, we used tubes fitted with 20 nm porous nylon membranes as surrogate models of reservoir-based implants. PBS was used as sink solution, with samples collected every 48 hours and analyzed via HPLC as detailed in the materials and methods.

To assess drug stability, we analyzed the purity of TAF_{fb} released into the sink solution. In contrast to literature approaches^{17–20}, we focused our attention on the analysis of the purity of the residual solubilized drug in the implant. The reasoning behind our approach is that an ideal implant should release unhydrolyzed TAF_{aq}, while maintaining stable drug within its reservoir. While analyzing the entire content of an implant reveals its internal composition, the purity of released TAF_{aq} remains unknown. Additionally, at any given time (except at the final phase of drug depletion), most TAF within an implant preserves its solid (unhydrolyzed) form due to its low aqueous solubility. As such, stability assessment via analysis of total residual drug in an implant can be confounding and does not inform on the proportion of TAF_{aq} and TFV*_{aq} released from the implant.

The results of our stability analysis for both TAF_{fb}- or TAF_{fs}-loaded implants are shown in Figure 4. Specifically, Figure 4 shows the % of non-degraded TAF_{fb} versus all tenofovir species released by the surrogate implants. While on day 4, all surrogate implants loaded with either TAF_{fb} or TAF_{fs} yielded high purity of released TAF_{aq}, where ~15% degradation was observed within the first 6 days of release, corresponding to a daily degradation rate of ~2.2%. Thereafter, a steep degradation profile was maintained for TAF_{fs}, with nearly 60% of purity lost in the released drug by day 30. Further, pH in the reservoirs loaded with TAF_{fs} was strongly acidic (3.9 – 4.1) due to fumaric acid, leading to rapid TAF degradation. Owing to its higher solubility, TAF_{fs} was released at a considerably higher rate as compared to TAF_{fb}. Because of this, surrogate implant reservoirs containing TAF_{fs} were depleted by day 30. In the case of TAF_{fb}, while the degradation process continued, a sharp reduction in slope was observed on day 6. Thereafter, an average daily degradation rate of 0.25% was observed for TAF_{fb}, corresponding to a degradation process nearly one-order-of-magnitude slower than TAF_{fs}.

This is consistent with the establishment of a saturated TAF_{aq} solution in the reservoir, followed by the acidification of the local environment due to hydrolysis of TAF_{fb}. As previously detailed, this process is self-inhibiting and slows down further hydrolysis, resulting in a change of degradation rate. In fact, analysis of the aqueous content of the reservoirs loaded with TAF_{fb} showed that pH was maintained at 6.4±0.1, in contrast with the sink solution pH of 7.4.

The aqueous solutions in TAF_{fs}-loaded reservoirs did not reach pH 3.6, as observed in the saturated solution. Similarly, the pH of TAF_{fb}-filled reservoir did not fall within the ‘stability window’ (below pH 6). Neither of these events occurred because of the neutralization effect of the sink solution (PBS at pH 7.4) with proton and anion exchange through the membrane. As such, it should be noted that changing membrane permeability to target specific TAF_{aq} rates may significantly affect trans-membrane ion exchange and ultimately impact the pH of the implant reservoir.

3.4 Excipients: in vitro assessment of *trans*-urocanic acid.

While solubility and dissolution rate of TAF_{fb} are adequate for implantable applications, excipients capable of maintaining the pH of aqueous solution in the implant within a “stability window” are needed. Typical buffers used to achieve pH values in the range 4.5 – 6 have a very high solubility in water. As an example, for citrate buffer, the solubility of citric acid at 37 °C is approximately 67% w/w (~4.4 M). High concentrations within the drug reservoir may result in high osmotic pressure that can damage an implant, especially those adopting polymeric reservoirs^{17–20}. Further, high concentrations of H⁺ donors and acceptors accelerates TAF hydrolysis. Most importantly, a significant difference in solubility between buffer and TAF leads to rapid buffer release and implant depletion. Under these circumstances, as the pH drifts outside of the “stability window”, the ability to stabilize TAF_{aq} is rapidly lost.

We sought to solve this problem by using a biocompatible molecule with a buffering capacity in the pH 4.5 – 6 window and with comparable solubility to TAF. While limiting our search to unimolecular buffers, we identified *trans*-urocanic acid (UA, ((2*E*)-3-(1*H*-

imidazol-4-yl)prop-2-enoic acid) as a candidate²⁹. In humans, UA is synthesized from histidine by deamination and is naturally found in the skin and liver³⁰. In the skin, UA functions as a natural ultraviolet (UV)-protectant by absorbing UVB light and converting from *trans*- to *cis*-form. Also, *cis*-UA has immunomodulating properties³¹ and was shown to reduce inflammation and inhibit skin or heart allograft rejection in rodents^{32,33}.

Co-dissolution in saline solution at 37 °C, showed solubility limits of 3.45±0.05 mg/mL and 6.97±0.15 mg/mL for UA and TAF_{fb}, respectively. The pH of this saturated solution was measured within the stability window of TAF_{fb} (pH 4.9). A TAF_{fb}-UA formulation was prepared by mixing finely-ground solid powders at a 2:1 ratio (w/w). The 2:1 ratio between TAF_{fb} and UA was adopted considering the solubility of both molecules in the mixture, and to ensure proportional depletion of TAF and UA from the implant reservoir. An in vitro TAF_{fb}-UA release experiment was performed using the same experimental setting as described previously for TAF_{fb} where surrogate implants with 20 nm nylon membrane were loaded with solid TAF_{fb}-UA formulation. The results showed that stability of released TAF_{aq} was maintained throughout the 9-month release study (Fig. 5). Specifically, unhydrolyzed TAF_{aq} accounted for 92±3% of released molecules predominantly throughout the study. Notably, a transient dip in stability was observed within the first 14 days of release, with a minimum TAF_{aq} purity of 84±8% measured at approximately one week from the beginning of the study. We attribute this transient occurrence to the slow solubilization of UA and the establishment of equilibrium in the aqueous phase within the drug reservoir. This is consistent with the release results obtained with TAF_{fb}. However, in the case of TAF_{fb}-UA formulation, purity rebounded by day 16 with nearly 99% of TAF_{aq}.

The pH values of the aqueous phase in the drug reservoir analyzed on days 8, 136, and 288 were 5.30±0.01, 5.40±0.07, and 5.80±0.56, respectively. This result confirmed that UA was able to preserve buffering capacity long-term, maintaining the pH within the “stability window”. However, on day 288, one of the surrogate implants (Fig. 1) was completely depleted of UA, and had a pH of 6.44, and 72.2% TAF_{fb} purity in the reservoir fluids, which negatively skewed the results. In light of UA depletion in one of the surrogate implants, the study was terminated for all other samples on day 288.

3.5 Evaluation of TAF_{fb}-UA formulation in vivo

TAF_{fb}-UA formulation was assessed in rhesus macaques (n=4) using flat, elongated Ti6Al4V implants mounted with a nanofluidic membrane with 150 nm nanochannels (Fig. 6A). Implants were similar to those previously adopted in our studies^{23,26,28} and further details are available in materials and methods and elsewhere^{23,26}. The objectives of this pilot in vivo assessment of TAF_{fb}-UA were: 1) to verify that the released TAF_{aq} could achieve preventive levels of TFV-DP in the PBMC for 35 days; 2) to verify that under in vivo conditions, UA could preserve the pH of the aqueous phase in the implant reservoir within the ‘stability window’; and 3) to confirm stability of TAF_{aq} and TAF_s in the implant. For this evaluation, implants were surgically inserted subcutaneously in the animal dorsum (Fig. 6A). Preventive TFV-DP PBMC levels were achieved within 3 days after implantation. We considered 100 fmol/10⁶ PBMC as the prevention target, conservatively exceeding the clinically protective level determined in the iPrEX trial^{2,17}. Thereafter, TFV-DP PBMC

levels were maintained at a median concentration of 228.0 fmol/10⁶ cells (IQR, 204.8 to 423.8 fmol/10⁶ cells) for 4 weeks (Fig. 6B), with all implants exceeding the preventive threshold. Sixty-three (63) days post-implantation, the implants were retrieved in a survival surgery. Based on the analysis of residual drug in the implants, the estimated average release rate for TAF (including degradation products) and UA was 1.44 and 0.90 mg/day, respectively. The pH of the aqueous phase inside the implant, measured immediately after explantation, was 5.48 ± 0.24 (Fig. 6C). This pH is remarkably close to the minimum K_H conditions and confirmed that UA was able to buffer the aqueous phase in the implant, maintaining it within the stability range. The analysis of aqueous phase showed that unhydrolyzed TAF_{aq} accounted for 78% (median) of the total amount of tenofovir-containing species present in the solution within the implant. The remaining fraction (~22%) consisted of TAF degradation products. In contrast, in a parallel study²⁶ we investigated TAFs-loaded implants in rhesus macaques and observed that after 1 and 4 months of implantation (28 and 112 days), average TAF stability in the liquid phase within the drug reservoir had decreased to 51.6% and 30.6%, respectively. Collectively, these results show that UA significantly limits TAF degradation and enhances TAF_{aq} stability.

Stability analysis of TAF in its solid form showed that TAF_s was preserved, with purity of 98±0.98% as measured via HPLC. This is consistent with other studies in the literature, which have shown that TAF in solid form is stable long-term. As the TAF_{fb}-UA formulation is a physical mixture, no effect of UA on altering TAF stability in solid state was expected.

By taking into account drug loading and estimated daily release of ~1.4 mg/day, the implants used in this study could in principle sustain TAF_{fb}-UA release for 215 days (~7 months). However, while the effective preventive subcutaneous daily dose of TAF has yet to be determined, our release rate largely exceeded the TFV-DP concentrations in PBMCs (100 fmol/10⁶ cells) conservatively considered as the benchmark prevention target²⁶. Notably, other studies are investigating different implantable devices targeting daily TAF releases lower than 1 mg/day¹⁷ and as low as 160 µg/day¹⁸. By considering release rates of 1 mg/day and 160 µg/day, our implant could nominally sustain TAF_{fb}-UA release for 300 days (~10 months) and ~5 years, respectively.

Conclusions

In this work, we investigated the parameters involved in the long-term stability of TAF_{fb} in reservoir-based implantable systems. Through in vitro analysis, we identified pH as the dominant factor affecting TAF_{fb} degradation via hydrolysis. Specifically, we determined a “stability window” in the range of pH 4.8 – 5.8 within which hydrolysis is significantly mitigated. To minimize TAF_{fb} degradation, pH 5.3 was found to be the optimal condition to maintain within the aqueous phase of an implant reservoir. We identified *trans*-UA as a potential buffer excipient; *trans*-UA has comparable solubility to TAF_{fb} and the ability to maintain a reservoir at approximately pH 5.4 in vitro. This is remarkably close to the optimal environmental conditions above. In contrast with rapid degradation observed for TAF fumarate salt and free base, UA preserved purity of released TAF_{fb} from an implantable reservoir above 90% for over 9 months. As a first assessment of the formulation in vivo in a relevant model, we performed a NHP study with subcutaneously implanted nanofluidic

implants loaded with TAF_{fb}-UA formulation. Preventive levels of TFV-DP in PBMC were achieved within 2 days post-implantation, and surpassed and maintained for the 35 days of analysis. Further, 2 months post implantation, analysis of the implant content showed that: 1) UA maintained the aqueous phase within the “stability window” at pH 5.48 ± 0.24 ; 2) TAF_{aq} and TAF_s stability were 78% and 98% (median), respectively. Overall, these results show that *trans*-UA represents a viable candidate to achieve TAF_{fb} stability in the context of LA HIV PrEP implantable or injectable systems. While reduction in UA content may be possible, this requires further analysis. Along with this, additional studies to assess potential effect of UA on solid TAF_{fb} stability, and the long-term safety, tolerability, and tissue response to sustained subcutaneous delivery of *trans*-UA in formulation with TAF_{fb} are warranted. Moreover, a thorough long-term PK investigation assessing levels of TAF_{fb} and TFV in plasma is required. These are focus of our next studies.

Acknowledgments

We thank Nicola Di Trani from the Houston Methodist Research Institute for image rendering and Simone Capuani for image design. We thank Luke Segura and Elizabeth Lindemann from the Michale E. Keeling Center for Comparative medicine and Research at UTMDACC for support in animal studies and Bharti Nehete for PBMC isolation. We thank Dr. Roberto Arduino for the useful discussions. We express our gratitude to Trevor Hawkins and James F. Rooney at Gilead for their support and helpful discussions. TAF was provided by Gilead Sciences. Funding: This work was supported by funding from the National Institutes of Health National Institute of Allergy and Infectious Diseases (R01AI120749; A.G.), the National Institutes of Health National Institute of General Medical Sciences (R01GM127558; A.G.). F.P.P. received funding support from Tecnológico de Monterrey and Consejo Nacional de Ciencia y Tecnología. Additional support from Frank J. and Jean Raymond Centennial Chair Endowment (A.G.). All authors declare no competing financial interest.

References

1. Grant RM et al. Preexposure Chemoprophylaxis for HIV Prevention in Men Who Have Sex with Men. 363, 2587–2599, doi:10.1056/NEJMoa1011205 (2010).
2. Anderson PL et al. Emtricitabine-tenofovir concentrations and pre-exposure prophylaxis efficacy in men who have sex with men. *Sci Transl Med* 4, 151ra125, doi:10.1126/scitranslmed.3004006 (2012).
3. Kamis KF et al. Same-Day HIV Pre-Exposure Prophylaxis (PrEP) Initiation During Drop-in Sexually Transmitted Diseases Clinic Appointments Is a Highly Acceptable, Feasible, and Safe Model that Engages Individuals at Risk for HIV into PrEP Care. *Open Forum Infect Dis* 6, ofz310, doi:10.1093/ofid/ofz310 (2019). [PubMed: 31341933]
4. Pinto RM, Lacombe-Duncan A, Kay ES & Berringer KR Expanding Knowledge About Implementation of Pre-exposure Prophylaxis (PrEP): A Methodological Review. *AIDS Behav* 23, 2761–2778, doi:10.1007/s10461-019-02577-7 (2019). [PubMed: 31292825]
5. Benítez-Gutiérrez L et al. Treatment and prevention of HIV infection with long-acting antiretrovirals. *Expert Review of Clinical Pharmacology* 11, 507–517, doi:10.1080/17512433.2018.1453805 (2018). [PubMed: 29595351]
6. Flexner C Antiretroviral implants for treatment and prevention of HIV infection. *Current opinion in HIV and AIDS* 13, 374–380, doi:10.1097/coh.0000000000000470 (2018). [PubMed: 29794816]
7. Spreen WR, Margolis DA & Pottage JC Jr. Long-acting injectable antiretrovirals for HIV treatment and prevention. *Current opinion in HIV and AIDS* 8, 565–571, doi:10.1097/coh.0000000000000002 (2013). [PubMed: 24100877]
8. Dolgin E Long-acting HIV drugs advanced to overcome adherence challenge. *Nature Medicine* 20, 323–324, doi:10.1038/nm0414-323 (2014).
9. Pons-Faudoa FP et al. 2-Hydroxypropyl-beta-cyclodextrin-enhanced pharmacokinetics of cabotegravir from a nanofluidic implant for HIV pre-exposure prophylaxis. *J Control Release* 306, 89–96, doi:10.1016/j.jconrel.2019.05.037 (2019). [PubMed: 31136811]

10. Pons-Faudoa FP, Ballerini A, Sakamoto J & Grattoni A Advanced implantable drug delivery technologies: transforming the clinical landscape of therapeutics for chronic diseases. *Biomed Microdevices* 21, 47, doi:10.1007/s10544-019-0389-6 (2019). [PubMed: 31104136]
11. Ferrati S et al. The nanochannel delivery system for constant testosterone replacement therapy. *J Sex Med* 12, 1375–1380, doi:10.1111/jsm.12897 (2015). [PubMed: 25930087]
12. Ferrati S et al. Leveraging nanochannels for universal, zero-order drug delivery in vivo. *J Control Release* 172, 1011–1019, doi:10.1016/j.jconrel.2013.09.028 (2013). [PubMed: 24095805]
13. Ray AS, Fordyce MW & Hitchcock MJ Tenofovir alafenamide: A novel prodrug of tenofovir for the treatment of Human Immunodeficiency Virus. *Antiviral research* 125, 63–70, doi:10.1016/j.antiviral.2015.11.009 (2016). [PubMed: 26640223]
14. Markowitz M et al. Phase I/II study of the pharmacokinetics, safety and antiretroviral activity of tenofovir alafenamide, a new prodrug of the HIV reverse transcriptase inhibitor tenofovir, in HIV-infected adults. *The Journal of antimicrobial chemotherapy* 69, 1362–1369, doi:10.1093/jac/dkt532 (2014). [PubMed: 24508897]
15. Mills A et al. Switching from tenofovir disoproxil fumarate to tenofovir alafenamide in antiretroviral regimens for virologically suppressed adults with HIV-1 infection: a randomised, active-controlled, multicentre, open-label, phase 3, non-inferiority study. *PLoS One* 16, 43–52 (2016).
16. Golla VM, Kurmi M, Shaik K & Singh S Stability behaviour of antiretroviral drugs and their combinations. 4: Characterization of degradation products of tenofovir alafenamide fumarate and comparison of its degradation and stability behaviour with tenofovir disoproxil fumarate. *Journal of pharmaceutical and biomedical analysis* 131, 146–155, doi:10.1016/j.jpba.2016.08.022 (2016). [PubMed: 27589032]
17. Gunawardana M et al. Pharmacokinetics of Long-Acting Tenofovir Alafenamide (GS-7340) Subdermal Implant for HIV Prophylaxis. *Antimicrobial Agents and Chemotherapy* 59, 3913–3919, doi:10.1128/AAC.00656-15 (2015).
18. Su JT et al. A Subcutaneous Implant of Tenofovir Alafenamide Fumarate Causes Local Inflammation and Tissue Necrosis in Rabbits and Macaques. *Antimicrobial Agents and Chemotherapy* 64, e01893–01819, doi:10.1128/AAC.01893-19 (2020).
19. Johnson LM et al. Characterization of a Reservoir-Style Implant for Sustained Release of Tenofovir Alafenamide (TAF) for HIV Pre-Exposure Prophylaxis (PrEP). *Pharmaceutics* 11, 315, doi:10.3390/pharmaceutics11070315 (2019).
20. Schlesinger E et al. A Tunable, Biodegradable, Thin-Film Polymer Device as a Long-Acting Implant Delivering Tenofovir Alafenamide Fumarate for HIV Pre-exposure Prophylaxis. *Pharm Res* 33, 1649–1656, doi:10.1007/s11095-016-1904-6 (2016). [PubMed: 26975357]
21. Safer D, Brenes M, Dunipace S & Schad G Urocanic acid is a major chemoattractant for the skin-penetrating parasitic nematode *Strongyloides stercoralis*. *Proc Natl Acad Sci U S A* 104, 1627–1630, doi:10.1073/pnas.0610193104 (2007). [PubMed: 17234810]
22. Wezynfeld NE, Goch W, Bal W & Fraczyk T cis-Urocanic acid as a potential nickel(II) binding molecule in the human skin. *Dalton Trans* 43, 3196–3201, doi:10.1039/c3dt53194e (2014). [PubMed: 24352502]
23. Di Trani N et al. Electrostatically Gated Nanofluidic Membrane for Ultra-Low Power Controlled Drug Delivery. *Lab on a Chip*, doi:10.1039/D0LC00121J (2020).
24. Di Trani N, Pimpinelli A & Grattoni A Finite-size charged species diffusion and pH change in nanochannels. *ACS Appl Mater Interfaces*, doi:10.1021/acsami.9b19182 (2020).
25. Bruno G et al. Unexpected behaviors in molecular transport through size-controlled nanochannels down to the ultra-nanoscale. *Nat Commun* 9, 1682, doi:10.1038/s41467-018-04133-8 (2018). [PubMed: 29703954]
26. Pons-Faudoa FP et al. Preventive efficacy of a tenofovir alafenamide fumarate nanofluidic implant in SHIV-challenged nonhuman primates. *bioRxiv*, 2020.2005.2013.091694, doi:10.1101/2020.05.13.091694 (2020).
27. Bushman LR et al. Determination of nucleoside analog mono-, di-, and tri-phosphates in cellular matrix by solid phase extraction and ultra-sensitive LC-MS/MS detection. *Journal of pharmaceutical and biomedical analysis* 56, 390–401, doi:10.1016/j.jpba.2011.05.039 (2011). [PubMed: 21715120]

28. Chua CYX et al. Transcutaneously refillable nanofluidic implant achieves sustained level of tenofovir diphosphate for HIV pre-exposure prophylaxis. *J Control Release* 286, 315–325, doi:10.1016/j.jconrel.2018.08.010 (2018). [PubMed: 30092254]
29. Zeng L et al. Tunable ionic transport control inside a bio-inspired constructive bichannel nanofluidic device. *Small* 10, 793–801, doi:10.1002/sml.201301647 (2014). [PubMed: 24031024]
30. Viiri J et al. Cis-urocanic acid suppresses UV-B-induced interleukin-6 and –8 secretion and cytotoxicity in human corneal and conjunctival epithelial cells in vitro. *Mol Vis* 15, 1799–1805 (2009). [PubMed: 19753313]
31. Norval M & El-Ghorr AA Studies to determine the immunomodulating effects of cis-urocanic acid. *Methods* 28, 63–70, doi:10.1016/s1046-2023(02)00210-4 (2002). [PubMed: 12231189]
32. Gruner S, Diezel W, Stoppe H, Oesterwitz H & Henke W Inhibition of skin allograft rejection and acute graft-versus-host disease by cis-urocanic acid. *J Invest Dermatol* 98, 459–462, doi:10.1111/1523-1747.ep12499855 (1992). [PubMed: 1548429]
33. Oesterwitz H, Gruner S, Diezel W & Schneider W Inhibition of rat heart allograft rejection by a PUVA treatment of the graft recipient. Role of cisurocanic acid. *Transpl Int* 3, 8–11, doi:10.1007/bf00333194 (1990). [PubMed: 2369484]

Highlights

- Tenofovir alafenamide (TAF) hydrolysis is minimal at pH 5.3.
- *Trans*-urocanic acid (UA) buffers TAF free base-loaded implant and sustains pH at ~5.4 in vitro and in vivo.
- TAF-UA formulation maintains TAF purity >90% in vitro for over 9 months.
- TAF-UA formulation in non-human primates preserves pH at 5.5 and TAF purity of >98% and >78% in solid and solvated forms, respectively.

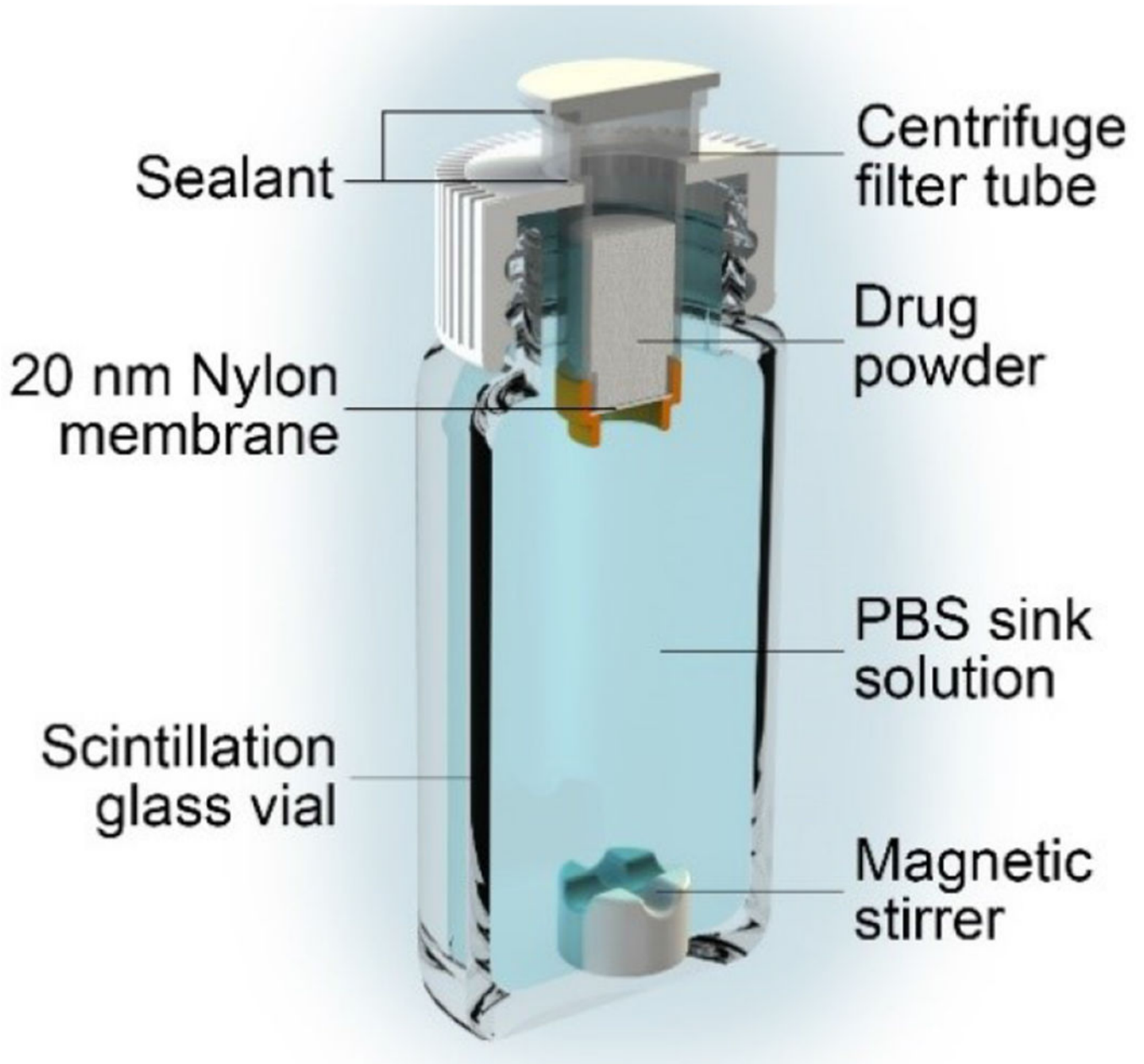


Figure 1. Experimental setup for in vitro release and stability evaluation using centrifugal filter tubes with 20 nm nylon membranes as implant surrogates.

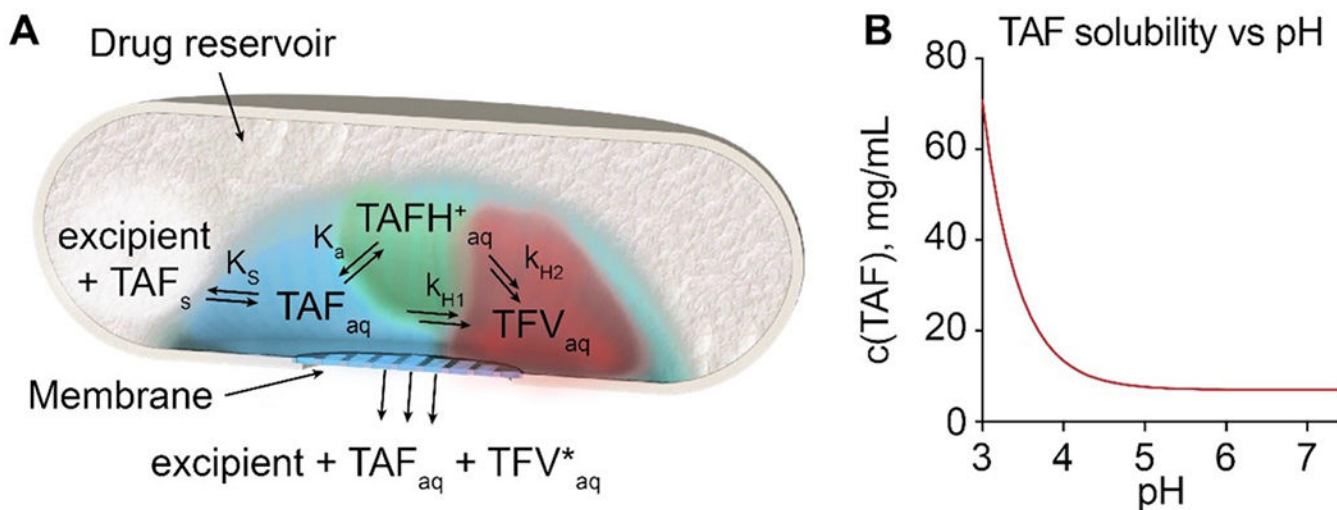


Figure 2.

(A) Schematics of TAF dissolution, degradation and release from a generic reservoir-based drug delivery implant. Solid TAF (TAF_s); dissolved TAF (TAF_{aq}); dissolved protonated TAF (TAH⁺_{aq}); dissolved tenofovir (TFV_{aq}); combined products of TAF hydrolysis (TFV^{*}_{aq}). k_s is TAF solubility constant, k_a is TAF acidity constant and k_{H1} , k_{H2} are the hydrolysis rate constants for neutral TAF and TAH⁺. (B) TAF solubility dependence on pH.

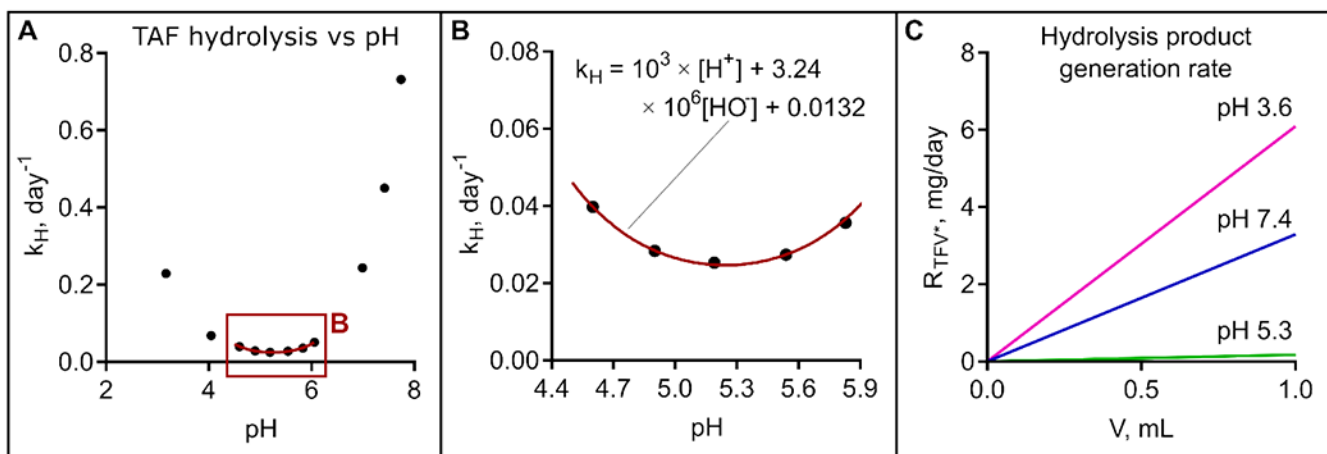


Figure 3.

(A) Hydrolysis rate k_H dependence on pH. (B) k_H fitting within 'stability window'. (C)

Hydrolysis product generation rate R_{TFV^*} at pH 3.6, corresponding to pH of solution saturated with TAF_{IS}, physiological conditions (pH 7.4), and at pH 5.3, corresponding to the minimum TFV* generation rate.

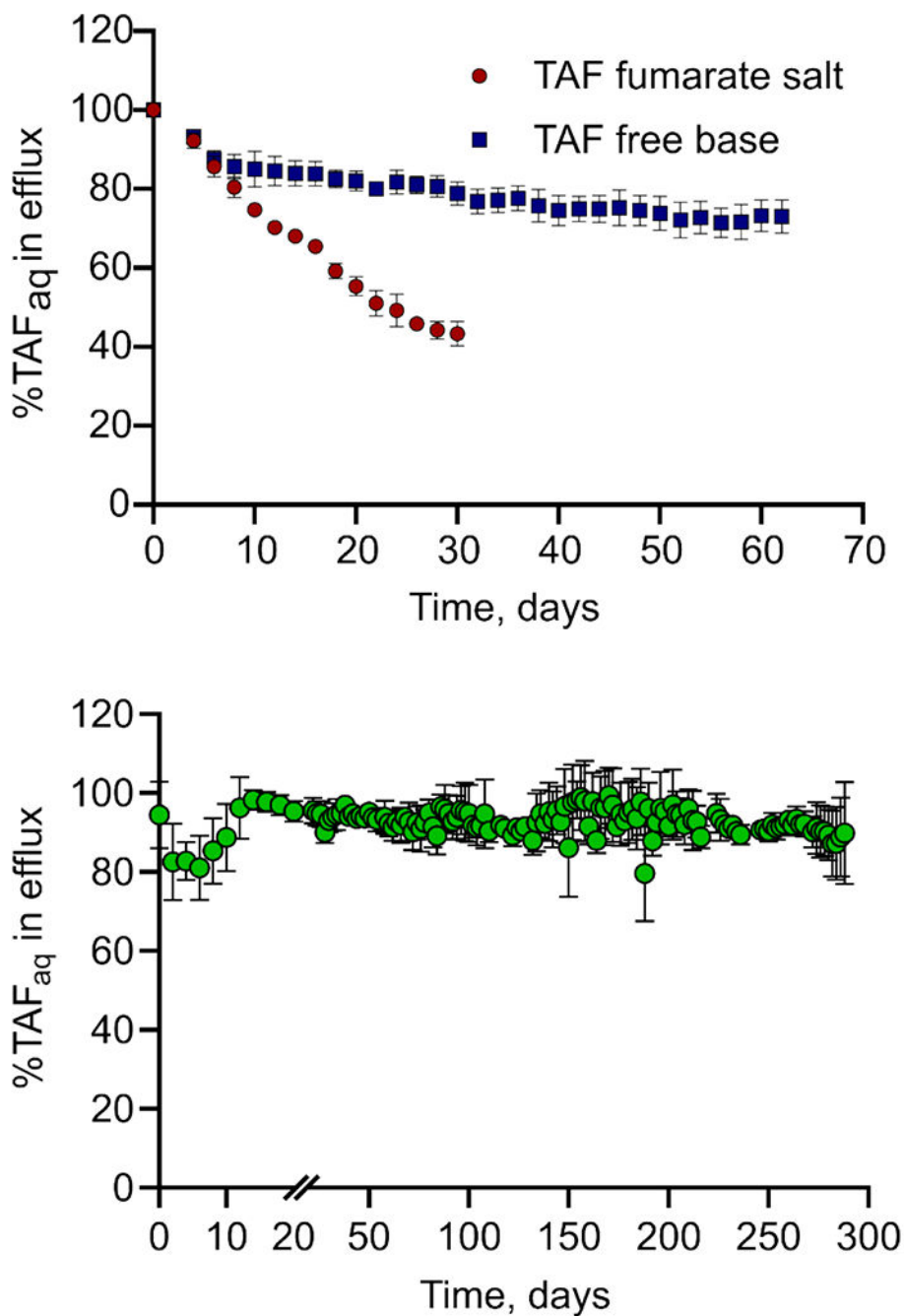


Figure 4. Percentage of stable TAF_{aq} released in vitro in sink solution from surrogate implants loaded with either TAF_{fb} or TAF_{fs}. Data are presented as mean±STD (n=5 replicates per group until day 44, n=4 thereafter).

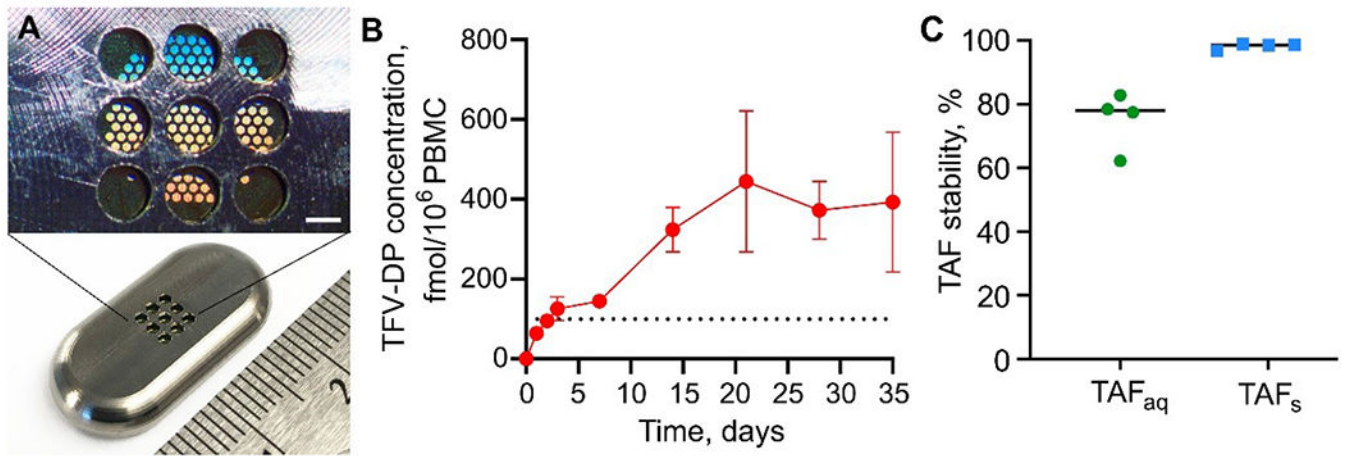


Figure 5. Percentage of stable TAF_{aq} released in vitro in sink solution from surrogate implants loaded with solid TAF_{fb}-UA formulation. Sink solution was collected, replaced and analyzed every 48h. Data are presented as mean±STD (n=3).

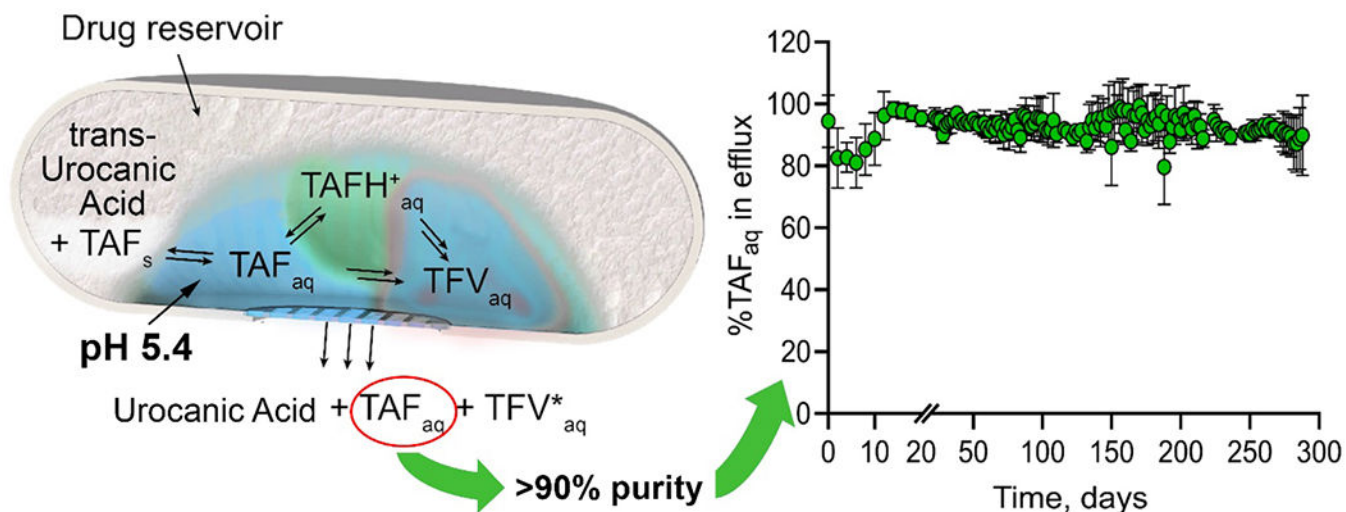


Figure 6.

TAF pharmacokinetics and stability in rhesus macaques implanted with subcutaneous TAF_{fb}-UA implants. Devices were retrieved after 63 days. (A) Medical-grade titanium implant (bottom) and magnification of the nanofluidic membrane and implant outlets (top; scale bar 200 μm). (B) Intracellular TFV-DP PBMC concentrations of TAF_{fb}-UA implants over 35 days. Data are presented as mean \pm SEM (n=4). Dotted black horizontal line at 100.00 fmol/ 10^6 cells indicate the threshold TFV-DP PBMC concentration that we adopted as the benchmark for prevention. (C) TAF_{aq} and TAF_S stability at time of implant removal on day 63. Horizontal lines represent the median.